Advanced Powder Technology 31 (2020) 4390–4400

Contents lists available at ScienceDirect

Advanced Powder Technology

journal homepage: www.elsevier.com/locate/apt

Original Research Paper

Green synthesis of gold nanoparticles using Parsley leaves extract and their applications as an alternative catalytic, antioxidant, anticancer, and antibacterial agents

Ola M. El-Borady [a,*], Mahmoud S. Ayat [b], Mostafa A. Shabrawy [b], Pierre Millet [c]

[a] Institute of Nanoscience and Nanotechnology, Kafrelsheikh University, Kafrelsheikh, Egypt
[b] Faculty of Biotechnology, October University for Modern Sciences & Arts (MSA), 6th October City, Egypt
[c] Institut de Chimie Moléculaire et des Matériaux d'Orsay, UMR 8182, Université Paris-Saclay, 91400 Orsay, France

ARTICLE INFO

Article history:
Received 30 May 2020
Received in revised form 18 August 2020
Accepted 16 September 2020
Available online 5 October 2020

Keywords:
Gold nanoparticles
Parsley
Antibacterial
Anticancer
Photo-catalytic

ABSTRACT

For the first time in this study, gold nanoparticles (AuNPs) were biosynthesized by the eco-friendly and cost-effective procedure using Presley leaf (Petroselinum crispum) extract then used as antioxidant, anticancer, antibacterial and photocatalytic agents. Different four-volume of the extract 2.5 mL, 5 mL, 10 mL, and 20 ML named AuNPs(A), AuNPs(B), AuNPs(C) and AuNPs(D) were used to module the size and shape of AuNPs. The prepared NPs were characterized by various techniques including UV–Vis absorption spectroscopy, Transmission Electron Microscopy (TEM), dynamic light scattering (EDX), and X-ray diffractometric (XRD). TEM imaging confirmed the formation of spherical, semi-rod aggregates, and flower-shaped NPs. The reduction and stabilization effect of the plant extract to fabricate AuNPs were explained by FTIR analysis. The four AuNPs provided high antioxidant ability, while AuNPs(D) was the best one. The NPs showed an emerging antimicrobial activity against two gram-negative microbes and not effective against the gram-positive microbes. The photocatalytic capacity for degradation of methylene blue dye was achieved after only one minute (the four samples have an equal effect). The AuNPs(D) provide the best anticancer activity on the human cancerous colorectal cell line using MTT assay rather than the other three AuNPs. The results spotlight for using Presley as a common cheap plant for bio-fabricating AuNPs who possess huge multifunctional applications.

1. Introduction

In recent years, AuNPs were among the most used nanostructures in several medical applications for diagnostic [1,2] and therapeutic [3,4]. They also showed high potential as antibacterial agents, those synthesized either chemically [5] or from plant extracts [6]. Various synthetic routes such as chemical reduction [2], photochemical reduction [7], electrochemical reduction [8], and heat evaporation [9] have been employed for the preparation of NPs. All these techniques produce metal NPs, but they are harmful to human beings and have several disadvantages, such as high process cost, high pressure, and a negative environmental impact due to the usage of many toxic organic substances. For this reason, there was a need to develop an eco-friendly process for the fabrication of the NPs. Thus, green chemistry approaches have already been developed for the production of many NPs [10,11], due to their simplicity, convenience, and eco-friendliness. The biogenic and green synthesis of AuNPs using plants [12–15], microorganisms [16], fungi [15] as well as algae [14] has been reported. The AuNPs-mediated plant extract was provided for its huge biological applications including antiparasitic [17], antioxidant [18], antibacterial [19], and anticancer [12] activities.

Parsley (Petroselinum crispum) is widely used as a garnish and green vegetable, a food flavor and employed for many medicinal purposes in various countries especially leaves that were utilized as an antitussive, gastrointestinal disorder, dermatitis, exanthema, macula, alphosis, hemorrhoid, kidney stone, otitis and diuretic [20,21].

In previous studies, Parsley was manipulated for the preparation of silver [22], ZnO [23], and Selenium [24] NPs. Parsley was found to be a rich source of iron and other minerals, vitamins (riboflavin, beta-carotene, thiamin, and vitamins E and C), volatile

* Corresponding author.
E-mail addresses: ola_elborady@nano.kfs.edu.eg, olachem_elborady@yahoo.com (O.M. El-Borady), mahmoud.ayat1999@gmail.com (M.S. Ayat), mostafa.ahmed26@msa.edu.eg (M.A. Shabrawy), pierre.millet@u-psud.fr (P. Millet).

https://doi.org/10.1016/j.apt.2020.09.017
0921-8831/

oils, and fatty acids. Subsequently, those bioactive compounds may serve as both reducing and stabilizing agents [25,26]. This was also confirmed by Chaves *et al.* [27] and Farzaei *et al.* [21], who detected that the aqueous extract of Parsley leaves contains the apigenin (4′,5,7,-trihydroxyflavone), cosmosiin (apigenin-7-O-glucoside), oxypeucedanin hydrate (coumarin 2″,3″-dihydroxyfuranocou marin), and apiinapigenin-7-O-apiosyl-(1 –〉 2)-O-glucoside) principally.

Hence, the present study was to utilize, for the first time a cheap procedure for the production of AuNPs using Parsley leaf extract without using other adding chemicals. The formation of NPs was evident from several spectral and microscopic tools. Furthermore, the efficiency of AuNPs for the reduction of the organic dye pollutant methylene blue (MB), was examined. Simultaneously, the antioxidant, antibacterial, and anticancer activity (against colon cells) of the synthesized AuNPs was also investigated.

2. Materials and method

2.1. Materials

The Parsley (Petroselinum crispum) leaves (Fig. 1**a**) were freshly collected from El Fayoum, Egypt. Gold (III) chloride tri-hydrate ($HAuCl_4{\cdot}3H_2O$) and 2,2-Diphenyl-1-picrylhydrazyl (DPPH) were obtained from Sigma-Aldrich. Methylene blue dyes (MB) and sodium borohydride ($NaBH_4$) were purchased from Loba Chemie, India. Deionized ultra-pure water (18 MΩ.cm) was used for preparing all respective solutions.

2.2. Preparation of aqueous Parsley extract

Parsley leaves were washed several times with de-ionized water to remove any dust, dried in the shade at room temperature to avoid denaturing any active principles. 20 gm of the dried leaves was stirred with 200 mL de-ionized water for 20 min at 90 °C. Next, the final solution was cooled and filtered through a Whatman No. 1 filter paper. A transparent, yellow color broth solution was obtained and kept at 4 °C for further use.

2.3. Biosynthesis of AuNPs by Parsley extract

The synthesis of AuNPs mediated by Parsley extract was based on the reduction of Au^{3+} to Au^0. Four different AuNPs samples were synthesized by using various amounts of the plant extract, 2.5 mL, 5 mL, 10 mL, and 20 mL, and the samples are denoted as AuNPs(A), AuNPs(B), AuNPs(C), and AuNPs(D), respectively with keeping the molarity of $HAuCl_4{\cdot}H_2O$ solutions at one mM in all solutions. In a typical experiment, an aqueous solution of 1 mM of $HAuCl_4{\cdot}3H_2O$ was placed in a clean Erlenmeyer flask, heated until boiling. At ebullition, the plant extract's desired volume was added and was left under vigorous stirring for two minutes. The colloidal solution's color changed upon the addition of the plant extract immediately (from yellow to blue, purple, green, and dark green for extract volumes 2.5 mL, 5 mL, 10 mL, and 20 mL, respectively), Fig. 1**b**, the color change confirms the formation of AuNPs (estimated concentration for each sample was 200 μg/L). The Parsley extract used in this method has a dual action: a reducing agent (that reduces Au^{3+} ions to Au^0) and a capping agent. The resulting colloidal solutions of bio-mediated AuNPs were then stored at 25 °C for further characterization and applications.

2.4. Characterization

The morphology of the synthesized NPs (including nanoscale, shape, and uniformity) was investigated by TEM microscope, (JEOL, model JEM-2010) with an accelerating voltage of 200 kV, equipped with Gatan Digital Camera (Model Erlangshen ES500), and their size distributions and Zeta-Potential were evaluated by DLS spectroscopy (Malvern Zetasizer Nano ZS90 analyzer at 25 °C). The optical absorbance of the as-prepared NPs solutions was measured by UV–Vis Spectrophotometer (Shimadzu UV-2450 spectrophotometer, one cm wide quartz cells). The structural information and types of functional groups from the extract that may be involved in the synthesis and stabilization of AuNPs were obtained by FTIR spectrophotometer (JASCO spectrometer) over the 4000 to 400 cm^{-1} range. The NPs samples were blended with potassium bromide (KBr) in a 1:100 ratio, compressed to a 2 mm disks using a designed screw knot. The elemental composition of powdered samples was determined by Energy-dispersive X-ray spectroscopy (EDX) using a JEOL model JSM-IT100 scanning electron microscope (SEM). The data on antioxidant properties were recorded on a Fluorescence Microplate Reader & Autosampler FP-8000 Series (JASCO).

2.5. The assessment of antioxidant efficiency

The free radical scavenging potential of the plant extract and prepared NPs were assessed using DPPH, according to Guntur et al. method [28]. Briefly, one mL of the as-synthesized AuNPs solution was mixed with 1000 μL of DPPH (0.2 mM). A DPPH solution without NPs was also examined and utilized as a negative control. Additionally, the test was also made on two-fold-diluted solutions of each sample. After that, the DPPH solutions were blended for 20 min at ambient temperature in a dark condition. At the end of the incubation period, the radical concentration was determined by following the reduction in its absorbance percentage at a specific wavelength of 517 nm. The scavenging

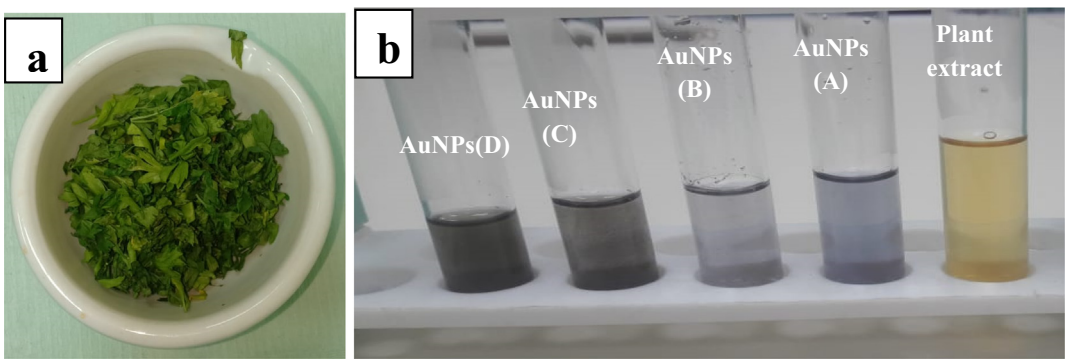

Fig. 1. (a) photo image for collected Parsley leaves; (b) photo image for the leaf extract and synthesized AuNPs.

efficiency was expressed as the inhibition percent of DPPH radicals, and it was calculated according to the following equation:

$$\text{Inhibition percent of DPPH radicals} = (\text{Control absorbance} - - \text{sample absorbance})/(\text{Control absorbance}) \times 100 \quad (1)$$

2.6. The antimicrobial assays

The in vitro antibacterial potential of the four bio-inspired suspensions AuNPs and the free plant extract was evaluated against four human pathogenic bacteria: two gram-positive bacterial strains *(Bacillus subtilis* and *Enterococci faecalis*) and two gram-negative bacterial strains *(Escherichia coli* and *Enterobacter ludwigii)* using Agar well-defined procedure. The solidified agar (Mueller Hinton Agar (MHA) plates were streaked for each bacterial strain's one-day culture. Subsequently, each plate was swept by using a sterilized cork borer to form wells (9 mm in diameter). Following that, 100 μL of an aqueous solution of each NPs sample was added into the created wells. The NPs solutions were left to diffuse into the agar for a few minutes, and then the plates were maintained carefully for 48 h incubation at 37 °C. After incubation, the zones of inhibition (the clear area around the wells) surrounding the discs indicated the antibacterial activity was measured in mm and tabulated.

2.7. The photocatalytic activity

The photocatalytic activity of AuNPs was assessed by investigating the reduction of MB dye via $NaBH_4$, whereas the biologically as-synthesized AuNPs were utilized as a catalyst at 25 °C under solar light. The procedure started by adding 2.5 mL of 0.08 mM MB dye solutions in a one cm path length quartz cuvette. Then, 0.5 mL of freshly prepared $NaBH_4$ (0.06 M) solution was added to the dye solution, followed by the addition of 0.5 mL of colloidal AuNPs. Afterward, the solution was subjected to solar light under gentle stirring. Another sample was prepared using the same procedure, but it was free from NPs (this sample was used as a reference to prove that the reduction was enhanced due to the presence of NPs). The dye's reduction reaction was monitored by recording changes in the MB absorption after one minute using the following equation:

$$\text{Degradation rate } (\%) = (C_0 - C)/C_0 \times 100 \quad (2)$$

While, C_0 = initial concentration of dye, C = the concentration of dye upon irradiation.

2.8. The anticancer studies

The MTT assay was used to determine the cytotoxic effect of the Parsley leaf extract and its four bio-synthesized AuNPs at various concentrations (200, 100, 50, 25, and 12.5 g/mL) on the human colorectal cell line.

2.8.1. Cell culture protocol

COLO- 201 colorectal colon, adenocarcinoma carcinoma cell line was delivered from Vascera cells and cultured using DMEM (Invitrogen/Life Technologies) supplemented with 10% FBS (Hyclone), 10 ug/mL of insulin (Gibco), and 1% penicillin–streptomycin (Gibco). All of the other chemicals and reagents were from Gibco, Germany. In a 96-well plate, a cell density with approximately 1.2 – 1.8 × 100,000 cells/well was completed by a volume of 200 μL of growth medium and + 200 μL of the tested materials for 24 h before the MTT assay.

2.8.2. Cell counting and cell viability 'Trypan blue' by hemocytometer

The total number of cells was determined by counting these cells with a hemocytometer. Briefly, ten of the harvested cells were added to the hemocytometer, and then the chamber was placed in an inverted microscope under a 10X objective. After that, the cells were counted and multiplied by 10^4 to estimate of the total number of cells per mL. Then, for every 0.1 mL of cells, 0.1 mL of trypan blue solution in buffer was added. To evaluate the total number of dead cells, the sample was loaded on the hemocytometer under low magnification, and the viable cells were counted using the following equation:

$$\% \text{ of viable cell} = [1.00 - - (\text{number of blue cells}/\text{Number of total cells})] \times 100 \quad (3)$$

The number of viable cells/mL of the culture was estimated by using the following formula: Number of viable cells 10^4 x1.1 = cells/mL culture

2.8.3. Cell cytotoxicity assay

The MTT assay was carried out using the *CellTiter 96* solution (Promega, Germany). An amount of 20 μL of CellTiter® AQueous one solution reagent was added over each well of the 96-well assay plate that was previously filled with 100 μL of culture medium. Afterward, all the plate was incubated for 1–4 h at 37 °C in a humidified incubator, under a 5% CO_2 atmosphere. At the end of the incubation period, the absorbance of the solutions was measured at a constant wavelength of 570 nm using a 96-well Plate Reader. Also, the IC_{50} value (concentration required to reach 50% inhibition of viability) was determined for each sample.

3. Results and discussion

3.1. Spectral, morphological, and structural characterization

3.1.1. Synthesis of AuNPs and UV–Visible spectroscopy

The green synthesis of AuNPs using environmental and non-toxic chemicals is the current approach. One of the most frequently used materials in green synthesis is the plant extract, which contains functional groups that can reduce Au^{3+} to Au^0. Since Parsley extracts contain several reducing groups, this may cause the formation and stabilization of AuNPs dispersions with quite diverse morphology. Through the current research, we study the influence of size and shape of NPs by changing the volume of leaf extract, thus, four plant extract volumes were applied for the reduction of Au^{3+} into Au^0.

The addition of Parsley extracts to $HAuCl_4$ aqueous solutions leads to rapid color changes of the mixtures, from light yellow to various ranges of colors from light purple to dark green, depending on the added amount of the plant extract. Obtaining different colors are reflecting the formation of NPs of different sizes and shapes. One of the most distinguishing features of metal NPs is their optical property. Furthermore, the formation of metal NPs can be ascertained by monitoring the appearance of the Surface Plasmon Resonance (SPR) band in the absorption spectrum of the aliquot of the metal NPs such as gold and silver NPs [29]. The position and shape of the SPR band depend on the morphology of the NPs [30]. Fig. 2 exposes the absorption spectra measured for the pure Parsley extract and the four colloidal solutions of AuNPs. The absorption spectrum of pure plant extract exhibited two sharp bands in the UV-region, centered at 266 nm and 336 nm, two values that are consistent with the findings of earlier studies [31] for Parsley. A distinguishable decrease in those two bands was recorded in the parsley-mediated AuNPs spectra, according to the amount of the used plant extract. Besides, the absorption spectra of the AuNPs(A), AuNPs(B), AuNPs(C), and AuNPs(D) showed the SPR bands at 547 nm, 572 nm, 627 nm, and 585 nm, respectively.

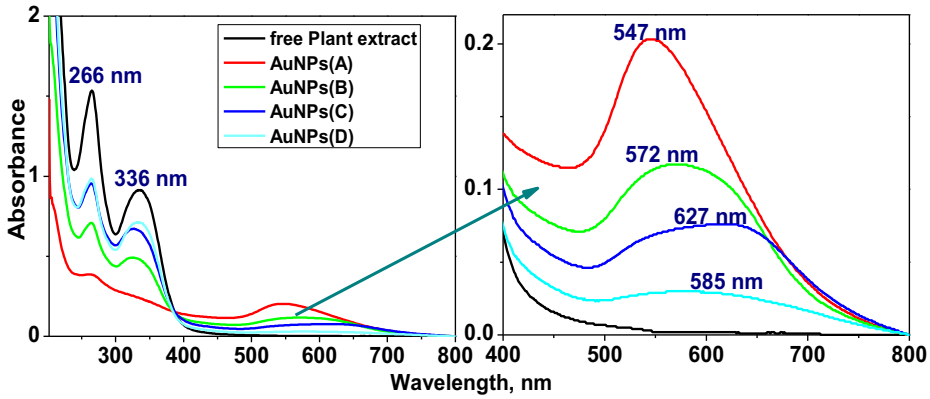

Fig. 2. UV-Visible absorption spectra for plant extract and the four synthesized colloidal solutions of AuNPs.

The increase in the extract volume resulted in the broadening of the SPR band, suggesting the formation of a broad distribution of NPs morphologies that was also detected by TEM analysis. Such results also coincided with previous results [32], which suggests the narrower SPR bands refer to the formation of smaller AuNPs in size, while broader SPR bands indicate a large size of AuNPs [33]. It was noticed that the AuNPs(C) spectrum looks as if two bands fused into each other, as previously seen for short rod-shaped NPs [30]. The frequent appearances of SPR at different wavelengths for the four NPs samples prove that they were in different sizes and shapes, which will be viewed in the TEM images.

3.1.1.1. High resolution Transmission electron microscope (HR-TEM). The morphological features of the fabricated AuNPs, such as shape and size, were observed by HR-TEM microscopy analysis. Fig. 3 (a), (b), (c), and (d) show the typical TEM images obtained for the AuNPs(A), AuNPs(B), AuNPs(C), and AuNPs(D) samples, respectively. The AuNPs(A) particles were found to be of uniform spherical shape, with a narrow size distribution centered at approximately 17 nm. The TEM images of AuNPs(B) show agglomerates of deformed spherical NPs, size between 20 and 40 nm. AuNPs(C) particles are multi-shaped with a size around 50 nm; also, most of the particles tend to be coupled and look like rods instead of spheres (similar information was deduced from the shape of the SPR band of this sample). Finally, AuNPs(D) showed agglomeration of small particle groups to form larger agglomerated particles with size (80 nm).

As a conclusion form TEM imaging, the most homogenous and has the best size distribution is AuNPs(A) that was prepared by the least amount of plant extract. The obtained results is matched with Lade, B.D., and Shanware [34], who advised using 1, 2, 3, 4, and 5 mL, since less volume is required for nanoscale particle synthesis. The diversity in particle shape and size is attributed to the difference in the amount of the plant extract added during the synthesis, this was confirmed by previously study for AuNPs prepared by Hibiscus rosa Sinensis [35].

The selected area electron diffraction (SAED) images of AuNPs(A), AuNPs(B), AuNPs(C), and AuNPs(D) were displayed in Fig. 3 (e), (f), (g), and (i), respectively, demonstrating their crystallinity [36].

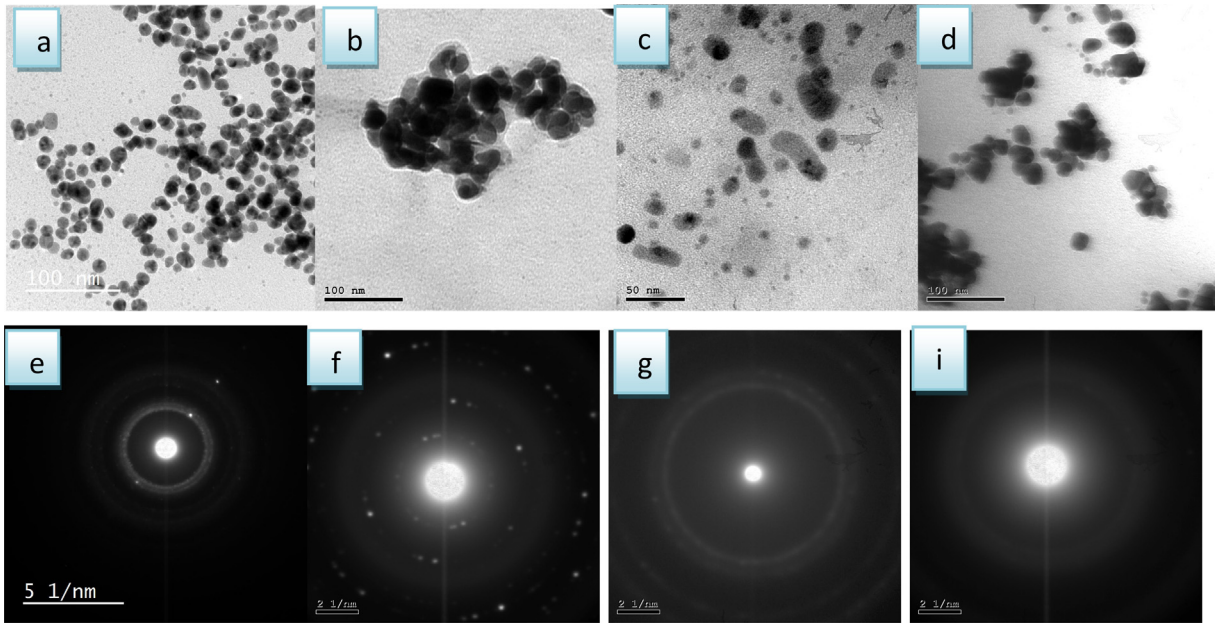

Fig. 3. (a–d): TEM images at different magnification scales and different spots for AuNPs(A), AuNPs(B), AuNPs(C), and AuNPs(D), respectively. (e–h): their diffraction pattern, respectively.

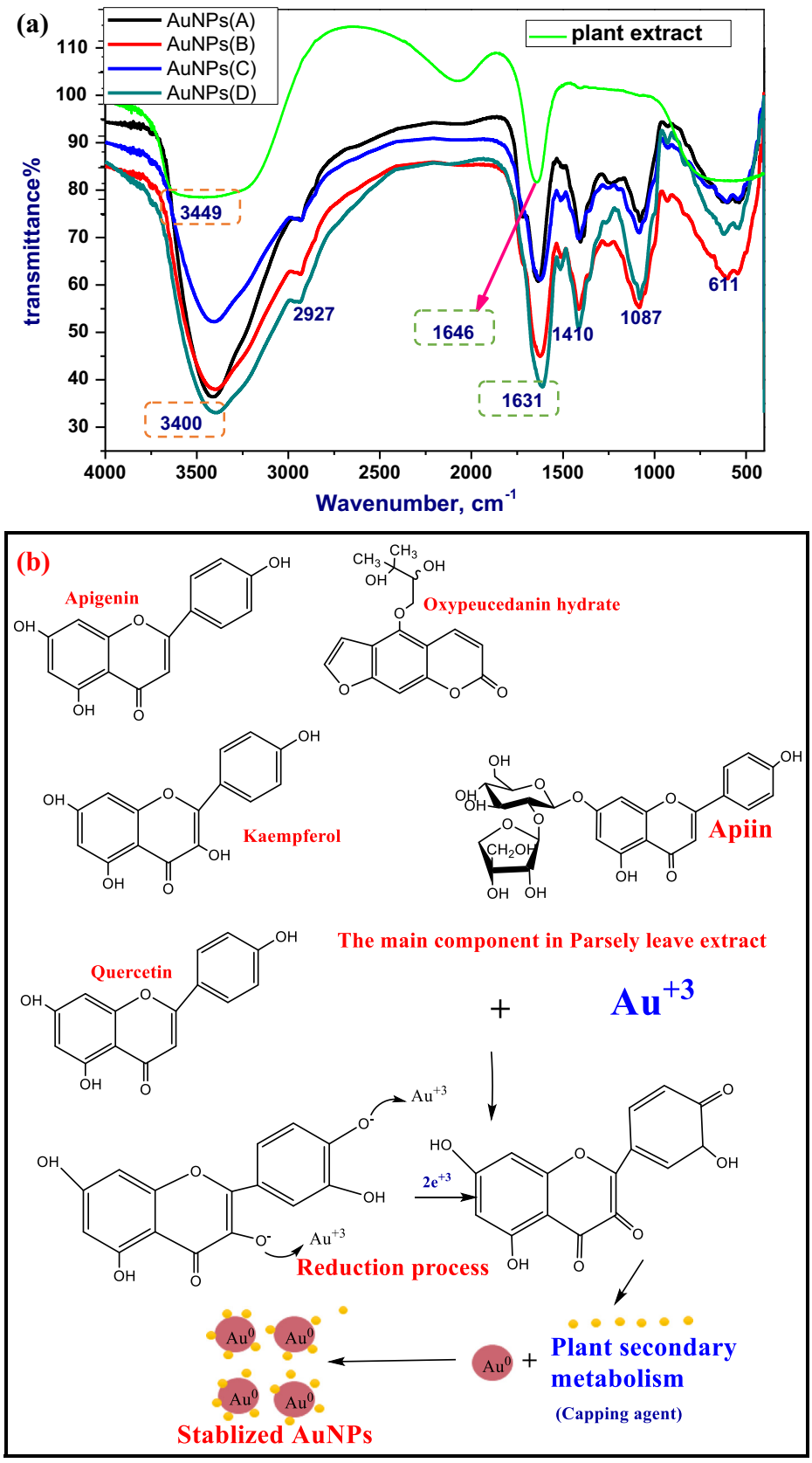

Fig. 4. a- The FTIR spectra for the free plant extract and synthesized AuNPs(A), AuNPs(B), AuNPs(C), and AuNPs(D), (b) the proposed mechanism for the reduction and stabilization of AuNPs by Parsley leave extract.

3.1.1.2. Energy dispersive X-ray microanalysis (EDX) analysis. EDX analysis of free plant and the four synthesized AuNPs represented in. Fig. 3 (a,b,c,d,e), supplementary information. The free plant EDX chart recorded several peaks attributed to carbon, oxygen, nitrogen, and potassium elements plus other minerals, as reported earlier for Parsley [37]. On the other hand, several identified strong lines corresponding to the gold element were detected for the major emission energies in all NPs samples, demonstrating the presence of AuNPs. Furthermore, weaker contributions due to carbon and nitrogen elements were detected, assigned to the residual plant biomolecules [38] that serve as capping agents for the AuNPs.

3.1.1.3. The fourier transformed infrared spectroscopy (FTIR). FTIR spectroscopy was used to identify the functional group and biomolecules available in the plant extract that has a role as reducers and stabilizers. Fig. 4**a**, the FTIR spectrum of the free extract contains major peaks located at 3449 cm^{-1} (O—H stretching vibration), 2927 cm^{-1} (C—H stretch), 1646 cm^{-1} (C-O symmetric stretch) [39], 1410 cm^{-1}, and 1085 cm^{-1} (C—N stretch vibration of aliphatic amines) [40]. The presence of functional groups like C-N, C—O, O—H, and N—H suggests the presence of flavonoids apigenin, quercetin, oxypeucedanin hydrate, cosmosiin, and apiin, as reported previously [21], in the aqueous extract of parsley leaves. It can be speculated that these moieties play the main role in the bioreduction of the process for gold ions [41] to form AuNPs. Moreover, in an earlier study, Li *et al.* [42] reported that the presence of the hydroxyl and carboxyl ions in biomolecules could develop protective layers at the surface of the NPs. Accordingly, such protective layers can help in the formation of stabilized NPs, and the plant can act as a stabilizing agent.

The FTIR spectra of the four AuNPs samples showed similar peaks at 3400 cm^{-1} (O—H stretching vibration), 2927 cm^{-1} (C-H stretch), 1631 cm^{-1} (C=O stretch), 1410 cm^{-1} (C—C stretch), 1085 cm^{-1} (C—N stretch vibration of aliphatic amines), and several other peaks in the 600–400 cm^{-1} range which is characteristic of metal bonds.

It was observed that the peak related to phenolic hydroxyl groups was shifted to lower wavelength values and was more intense in the four NPs than in the free plant extract. This may be ascribed to the binding of AuNPs to the plant's surface through OH moieties present in the plant. Furthermore, the C=O stretch bands were relatively blue-shifted, indicating a possible linkage to Au particles via hydrogen bonds of these groups. Subsequently, it is concluded from the FTIR analysis that gold ions were reduced via the plant extract and bound to it through OH and/or C=O groups Fig. 4**b**.

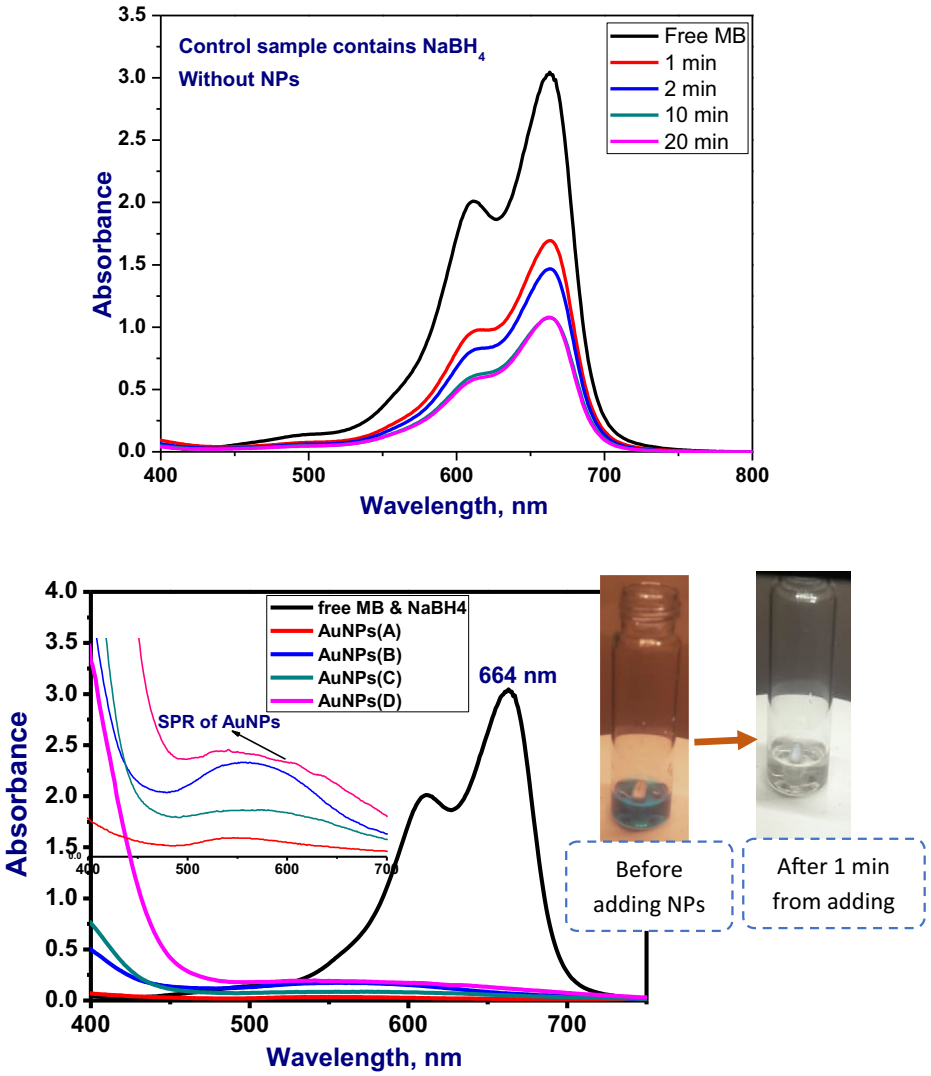

Fig. 5. Absorbance spectra of photo degradation for MB dye in the presence of AuNPs(A), AuNPs(B), AuNPs(C), and AuNPs(D) and control sample with $NaBH_4$ only; last photo image for solution before adding NPs and one minute after the addition of NPs.

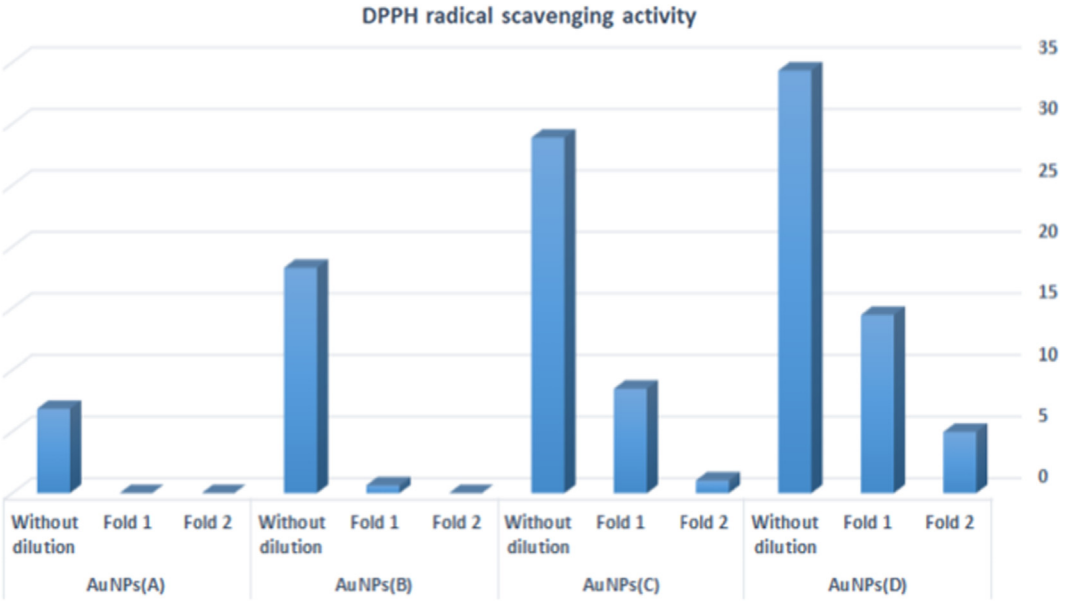

Fig. 6. The DPPH radical scavenging activity of synthesized AuNPs(A), AuNPs(B), AuNPs(C), and AuNPs(D).

3.1.2. Zeta-Potential and dynamic light scattering analysis

The zeta potential was performed to measure the colloidal stability and surface charge of the synthesized AuNPs. The zeta potentials of AuNPs(A), AuNPs(B), AuNPs(C), and AuNPs(D) are −15.4, −8.75, −19.5 and −6.56 mV, respectively, Fig. 2 supplementary information. These highly negative zeta potential values describe the presence of the bioactive compounds with a negative charge on the NPs surface, providing an efficient stabilization of Bio-AuNPs [43], which is also matched with the IR findings [44].

The DLS was used to determine the particle size distributions, this technique is based on the measurement of the time-dependent fluctuations of the scattering of light by NPs undergoing the Brownian movement [45]. The DLS AuNPs(A), AuNPs(B), AuNPs (C), and AuNPs(D) are 134, 110, 840 and 712 nm, respectively, diagrams Fig. 3 supplementary information. The polydispersity (PDI) was found to be 0.509, 1.0, 0.868, and 0.620 for AuNPs(A), AuNPs(B), AuNPs(C), and AuNPs(D), respectively. According was to AuNPs(A) sample displayed the highest polydispersity.

3.2. The AuNPs Photocatalytic potential for reduction of methylene blue (MB)

The water treatment from contamination with organic dyes is a formidable challenge nowadays. We selected MB for our study because MB is one of the most used organic dyes in many industries, and its residual in wastewater is considered as toxic

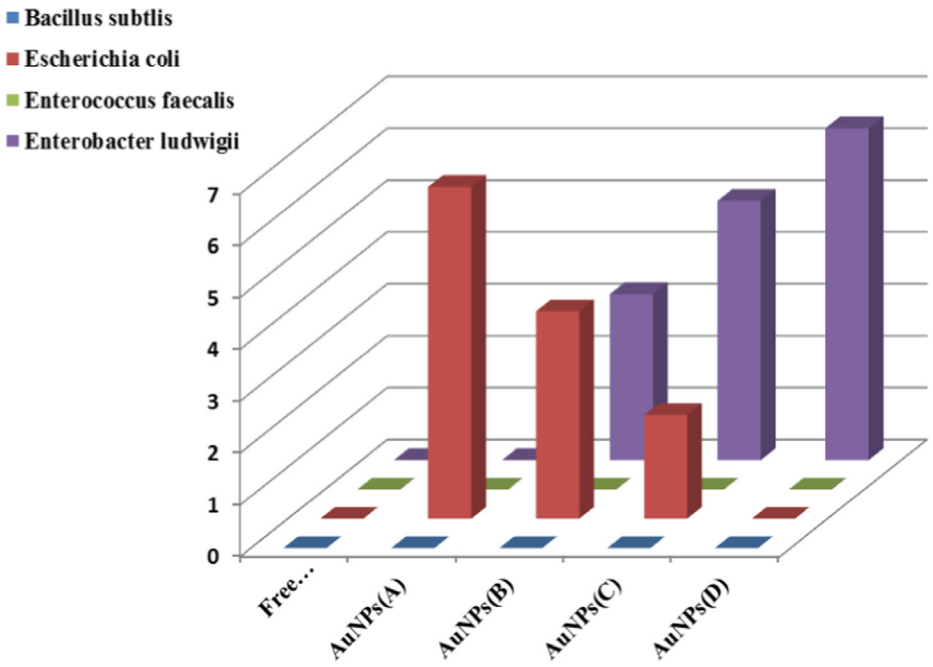

Fig. 7. The zones of inhibition against different bacterial strains of AuNPs(A), AuNPs(B), AuNPs(C), and AuNPs(D).

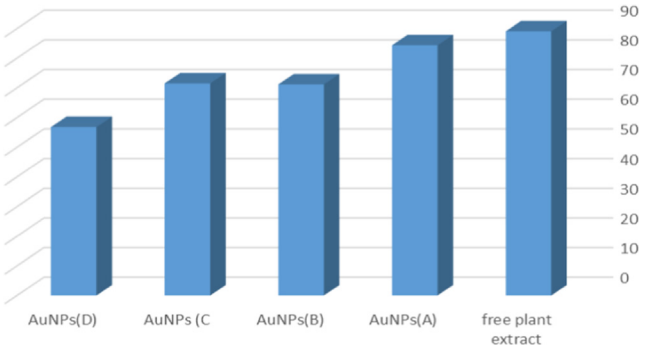

Fig. 8. Cell viability (%) of the plant extract and AuNPs(A), AuNPs(B), AuNPs(C), and AuNPs(D) on human colorectal cancerous cell line.

contamination. The MB was extensively used in the industry as a redox indicator [46,47] and the traditional tools to withdraw it from wastewater was to use a reducing agent such as $NaBH_4$ that generates hydrogen gas by a hydrolysis reaction in aqueous solution. The present study examines the catalytic activity of AuNPs in the presence of $NaBH_4$. It is well known that the absorption spectrum of MB has a λ_{max} value at 664 nm ascribed to the $n - \pi^*$ transition and another shoulder peak at 614 nm [48]. This peak decreases gradually in the presence of $NaBH_4$ due to the formation of the reduced form called leucomethylene blue (LMB) [49]. Nevertheless, it was found that the reduction rate by $NaBH_4$ was prolonged and it took time. AuNPs have been used as catalyzing agents in recent studies because they can reduce the redox potential to more negative values [50,51] to enhance and facilitate the transfer of electrons (e^-) from BH_4^- ions to the MB dye to form LMB [52]. We investigated the MB reduction in the presence of $NaBH_4$ and green-fabricated AuNPs by monitoring the degradation of the absorption peak at 664 nm. The resulting absorption spectra is plotted in Fig. 5. It was observed that upon the addition of any sample from four prepared AuNPs to the MB and $NaBH_4$ solution, the solution's blue color disappeared. The intensity of the peak at 664 nm completely disappeared after one minute and only the SPR band of AuNPs appeared (inset of Fig. 5), confirming that the AuNPs served as an active catalyst for MB reduction. This matched with early obtained [53]. Following the control sample ($NaBH_4$ solution without any AuNPs), a 65% reduction was obtained after ten minutes and it remained unchanged for 20 min. Accordingly, a clear improvement and enhancement were obtained due to the addition of the AuNPs (the four samples have equal catalytic effect towards MB degradation).

3.3. The antioxidant activity

It was reported that during numerous biological processes, a reactive oxygen species and other free radicals might be formed and released, causing pathogenicity [54,55]. The antioxidant activity is a concept referring to the formation of non-reactive and stable radicals through the inhibition process of the oxidation of any molecules. This is achieved by preventing the initiation step in the oxidative chain reactions. Therefore, much effort was implemented to find an antioxidant agent that obstructs or prevents this oxidative damage [56]. It was shown recently that AuNPs have significant antioxidant potential, especially those prepared via a green method [38,57,58] and it depends on the properties of various phytochemicals encrusted at the surface of the NPs [59]. Herein, the antioxidant capability of the biosynthesized AuNPs samples (as prepared and after dilution) was estimated using DPPH (Fig. 6). All AuNPs samples were found to possess good quenching for DPPH radical scavenging activity when used as it is or after dilution. Furthermore, the maximum percentage achieved was ordered as AuNPs(D), AuNPs(C), AuNPs(B), and the lowest value was for AuNPs(A); that is, as the volume of the mediated plant increased, the antioxidant effect increased. When the NPs were diluted to one fold, their antioxidant activity was retained. However, after a two-fold dilution, only samples AuNPs(C) and AuNPs(D) showed a low percentage of inhibition (the antioxidant activity of AuNPs was dose-dependent).

The antioxidant activity of synthesized AuNPs may be attributed to their secondary metabolite, including fiber, Apiin compound, essential oil, and different phenolic, flavonoid moieties found in the plant extract. As shown before Fig. 4, those substances may bind to the AuNPs surface as capping agents and provide an excellent antioxidant activity [60]. Furthermore, Tang et al., [61] discussed the scavenging potential of Parsley extract and attributed this activity due to the presence of phenolic compounds in Parsley, since these compounds can readily donate hydrogen atoms to the radical. Moreover, Farzaei, et al [21], attributed the antioxidant activity of the Parsley leaves due to the Apigenin compounds that are considered as the main component in leaves. The antioxidant effect of the currently prepared AuNPs from Parsley could be utilized in various applications such as natural health prevention [62].

3.4. Antimicrobial activity

The synergistic in vitro antibacterial activity of the four fabricated bio-mediated samples (AuNPs(A), AuNPs(B), AuNPs(C), and AuNPs(D)) compared to the free plant extract was put into evidence against four pathogenic microbial strains including two gram-positive (*Bacillus subtilis* and *Enterococci faecalis*) and two gram-negative bacteria *(Escherichia coli* and *Enterobacter ludwigii)*. The antibacterial efficacies were investigated by evaluating the mean inhibition zone (mm) that was tabulated in Table 1 supplementary information and drawn in Fig. 7. It has been demonstrated that metal NPs such as silver and AuNPs [63,64] exhibit anticandida and microbial potential, especially those synthesized by using a green process [65] whereas the antimicrobial activity is dependent on the method of synthesis, shape, size and concentration of the generated NPs [66]. They can severely inhibit a lot of pathogenic strains, by interfering constructively with bacteria via different mechanisms; (1) antibacterial mechanism through direct contact occurs by adhesion of NPs onto the surface of the cell wall and penetration to it and (2) ion-mediated killing [67].

As presented in Fig. 7, the plant extract alone was inert and had no activity to prevent the growth of the different examined bacterial strains. However, AuNPs were active only against tested gram-negative bacteria. AuNPs(A) has prevented the growth of only one of the tested bacteria *(Escherichia coli)* (a significant zone of inhibition close to 6.4 mm was measured). AuNPs(B) and AuNPs(C) were found active against *Escherichia coli* and *Enterobacter ludwigii* (inhibition zones of 4 mm, 2 mm and 3.2 mm, 5 mm, respectively). Furthermore, AuNPs(D) were found active against *Enterobacter ludwigii* (a 6.4 mm zone was measured), which was higher than the activity of AuNPs(B) and AuNPs(C). None of the fabricated AuNPs showed any inhibition activity against tested gram-positive bacteria strains. This was attributed to the fact that the gram-negative bacteria possess a thinner cell wall in comparison to the gram-positive bacteria as rigid peptidoglycan layers on its surface that preventing the entering of the NPs, so the AuNPs have a durable electrostatic attractiveness towards the negatively charged bi-layer, thereby facilitating the diffusion of AuNPs and cell lysis [68]. Similar results were observed on AuNPs prepared using Solanum nigurum leaves [67]. In the present study, the antibacterial inhibition mechanism by biosynthesized AuNPs may start by binding the polyphenols present in the extract with the protein that exists in the microbes. It changes the membrane

potential then reduces the synthase activity of adenosine triphosphate. Hence, the metabolism process gets reduced. Secondly, the biological mechanism is collapsed by declining the subunit of the ribosome for tRNA binding. The capping agent's binding feature supports the insertion of metal NPs to the inner core of the cells of microbes. At the same moment, they proved to be less toxic to mammal cells, which makes the green synthesis a remarkable one [69].

3.5. Cytotoxicity assessment

Previous reports suggested that AuNPs fabricated by green processes maintain the significant capacity to suppress the growth of the cancerous cells and were potent to work as bio-medical anticancerous agents [12,70]. This is why we investigated the in vitro cytotoxicity of the four green synthesized AuNPs samples and compared them to the activity of the pure plant extract through MTT assay on human colorectal cell line (CO-II). In a typical experiment, the CO-II cells were continuously exposed to different concentrations of samples (200, 100, 50, 25 and 12.5 g/mL) for 44 h. The percentage of the viable cells was found to decrease in proportion to the volume of the sample used. The cytotoxicity results obtained by measuring the OPD were tabulated in **Table 2** supplementary information. The percentage of cell viability of the different samples was plotted in Fig. 8. The 50% minimum inhibitory concentration (IC_{50}) was determined as 89.1, 56.83, 71.51, 71.16, and 84.39 for the pure plant extract and AuNPs(A), AuNPs(B), AuNPs(C), and AuNPs(D), respectively. The highest cytotoxicity was provided by AuNPs(A) may be due to its tiny size. Typically, smaller NPs have high anticancer effect due to the larger surface area of smaller NPs.These results evidenced a remarkable and strong therapeutic anticancer potential of the synthesized NPs. In 2018, Khalil *et al.* [71] attributed the cytotoxicity effect of the green synthesized AuNPs to the generation of free radicals (ROS). A similar activity was achieved when treating HEK293 cell lines using AuNPs [12].

4. Conclusion

In summary, AuNPs were successfully biosynthesized by an inexpensive, fast, and safe approach, using Parsley leaves, without the use of any toxic chemicals. Four different AuNPs samples were prepared using different volumes of the plant extract. EDX achieved the formation and presence of AuNPs. Besides that, TEM imaging revealed that these AuNPs have spherical, semi-rod, or flower shapes, depending on the amount of the extract used while AuNPs (A) has the most homogeny in size and shape and highest polydispersity as detected from DLS. Moreover, FTIR analysis suggested that the surface of AuNPs is covered by biomolecules found in the plant extract such as protein and polyphenols. These species contribute to the stabilization of the NPs as confirmed from the negative charges detected from zeta potential. These AuNPs have demonstrated an excellent catalytic activity for the degradation of MB. Additionally, AuNPs(D) displayed the most potent antioxidant potential. Also, an antibacterial inhibition was evident against two gram-negative pathogenic. Furthermore, AuNPs(A) has proven the best anticancer efficiency towards human colon cancer cells (HCT116). The overall results demonstrate the potential of such multifunctional NPs to be used in a wide spectrum of biomedical applications.

Declaration of Competing Interest

The authors declare that they have no known competing financial interests or personal relationships that could have appeared to influence the work reported in this paper.

Acknowledgements

The authors gratefully acknowledge Prof. Dr. Ayman Diab and Prof. Dr. Gehan Safwat (Faculty of Biotechnology, October University for Modern Sciences & Arts (MSA), Egypt) for their support; Dr. Mohamed El Dawody and Dr. Aman Allah Zaky for TEM imaging; Miss. Heba T. Zaher, Research lab, MSA University and Prof. Dr. Nashwa EL-Khazragy, Prof. clinical Pathology/Hematology and Biomedical Research departments, Faculty of Medicine, Ain Shams University, Cairo, Egypt.

Authors' contributions

Ola El Borady, designed the experiment, prepare NPs and photodegradation, conducted the spectral analysis, illustrate the whole data, and in writing the manuscript. **Mostafa and Mahmoud** participated in preparing NPs and antimicrobial study. **Pierre Millet** revise the manuscript writing.

Financial support

The current research didn't receive any fund.

Appendix A. Supplementary material

Supplementary data to this article can be found online at https://doi.org/10.1016/j.apt.2020.09.017.

References

[1] F. Fatemi, S.M. Amini, S. Kharrazi, M.J. Rasaee, M.A. Mazlomi, M. Asadi-Ghalehni, M. Rajabibazl, E. Sadroddiny, Construction of genetically engineered M13K07 helper phage for simultaneous phage display of gold binding peptide 1 and nuclear matrix protein 22 ScFv antibody, Colloids Surf. B 159 (2017) 770–780.
[2] A.M. Smith, H. Duan, M.N. Rhyner, G. Ruan, S. Nie, A systematic examination of surface coatings on the optical and chemical properties of semiconductor quantum dots, PCCP 8 (2006) 3895–3903.
[3] A.A.K. Zarchi, S.M. Amini, A. Salimi, S. Kharazi, Synthesis and characterisation of liposomal doxorubicin with loaded gold nanoparticles, IET Nanobiotechnol. 12 (2018) 846–849.
[4] S.M. Amini, S. Kharrazi, M.R. Jaafari, Radio frequency hyperthermia of cancerous cells with gold nanoclusters: an in vitro investigation, Gold Bull. 50 (2017) 43–50.
[5] E. Darabpour, N. Kashef, S.M. Amini, S. Kharrazi, G.E. Djavid, Fast and effective photodynamic inactivation of 4-day-old biofilm of methicillin-resistant Staphylococcus aureus using methylene blue-conjugated gold nanoparticles, J. Drug Delivery Sci. Technol. 37 (2017) 134–140.
[6] A.I. El-Batal, A.-A.-M. Hashem, N.M. Abdelbaky, Gamma radiation mediated green synthesis of gold nanoparticles using fermented soybean-garlic aqueous extract and their antimicrobial activity, SpringerPlus 2 (2013) 129.
[7] K. Mallick, M.J. Witcomb, M.S. Scurrell, Self-assembly of silver nanoparticles in a polymer solvent: formation of a nanochain through nanoscale soldering, Mater. Chem. Phys. 90 (2005) 221–224.
[8] Y.-C. Liu, L.-H. Lin, New pathway for the synthesis of ultrafine silver nanoparticles from bulk silver substrates in aqueous solutions by sonoelectrochemical methods, Electrochem. Commun. 6 (2004) 1163–1168.
[9] C.H. Bae, S.H. Nam, S.M. Park, Formation of silver nanoparticles by laser ablation of a silver target in NaCl solution, Appl. Surf. Sci. 197 (2002) 628–634.
[10] P. Raveendran, J. Fu, S.L. Wallen, Completely "green" synthesis and stabilization of metal nanoparticles, J. Am. Chem. Soc. 125 (2003) 13940–13941.
[11] K. Chand, D. Cao, D.E. Fouad, A.H. Shah, A.Q. Dayo, K. Zhu, M.N. Lakhan, G. Mehdi, S. Dong, Green synthesis, characterization and photocatalytic application of silver nanoparticles synthesized by various plant extracts, Arabian J. Chem. (2020).
[12] M.P. Patil, X. Jin, N.C. Simeon, J. Palma, D. Kim, D. Ngabire, N.-H. Kim, N.H. Tarte, G.-D. Kim, Anticancer activity of Sasa borealis leaf extract-mediated gold nanoparticles, Artif. Cells Nanomed. Biotechnol. 46 (2018) 82–88.
[13] S. Iravani, Green synthesis of metal nanoparticles using plants, Green Chem. 13 (2011) 2638–2650.
[14] T.S. Dhas, V.G. Kumar, L.S. Abraham, V. Karthick, K. Govindaraju, Sargassum myriocystum mediated biosynthesis of gold nanoparticles, Spectrochim. Acta Part A Mol. Biomol. Spectrosc. 99 (2012) 97–101.

[15] S.K. Das, C. Dickinson, F. Lafir, D.F. Brougham, E. Marsili, Synthesis, characterization and catalytic activity of gold nanoparticles biosynthesized with Rhizopus oryzae protein extract, Green Chem. 14 (2012) 1322–1334.
[16] P. Manivasagan, S.Y. Nam, J. Oh, Marine microorganisms as potential biofactories for synthesis of metallic nanoparticles, Crit. Rev. Microbiol. 42 (2016) 1007–1019.
[17] S. Rahul, P. Chandrashekhar, B. Hemant, S. Bipinchandra, E. Mouray, P. Grellier, P. Satish, In vitro antiparasitic activity of microbial pigments and their combination with phytosynthesized metal nanoparticles, Parasitol. Int. 64 (2015) 353–356.
[18] A. Lakshmanan, C. Umamaheswari, N. Nagarajan, A facile phyto-mediated synthesis of gold nanoparticles using aqueous extract of Momordica cochinchinensis rhizome and their biological activities, J. Nanosci. Technol. (2016) 76–80.
[19] D. MubarakAli, N. Thajuddin, K. Jeganathan, M. Gunasekaran, Plant extract mediated synthesis of silver and gold nanoparticles and its antibacterial activity against clinically isolated pathogens, Colloids Surf., B 85 (2011) 360–365.
[20] M. Aghili, Makhzan-al-advia, Tehran: Tehran University of Medical Sciences, 328 (2009).
[21] M.H. Farzaei, Z. Abbasabadi, M.R.S. Ardekani, R. Rahimi, F. Farzaei, Parsley: a review of ethnopharmacology, phytochemistry and biological activities, J. Tradit. Chin. Med. 33 (2013) 815–826.
[22] K. Roy, C. Sarkar, C. Ghosh, Plant-mediated synthesis of silver nanoparticles using parsley (Petroselinum crispum) leaf extract: spectral analysis of the particles and antibacterial study, Appl. Nanosci. 5 (2015) 945–951.
[23] M. Stan, A. Popa, D. Toloman, A. Dehelean, I. Lung, G. Katona, Enhanced photocatalytic degradation properties of zinc oxide nanoparticles synthesized by using plant extracts, Mater. Sci. Semicond. Process. 39 (2015) 23–29.
[24] L. Fritea, V. Laslo, S. Cavalu, T. Costea, S.I. Vicas, GREEN BIOSYNTHESIS OF SELENIUM NANOPARTICLES USING PARSLEY (PETROSELINUM CRISPUM) LEAVES EXTRACT, Studia Universitatis" Vasile Goldis" Arad, Seria Stiintele Vietii (Life Sci. Series) 27 (2017) 203–208.
[25] A.K. Mittal, Y. Chisti, U.C. Banerjee, Synthesis of metallic nanoparticles using plant extracts, Biotechnol. Adv. 31 (2013) 346–356.
[26] K. Mukunthan, S. Balaji, Cashew apple juice (Anacardium occidentale L.) speeds up the synthesis of silver nanoparticles, Int. J. Green Nanotechnol. 4 (2012) 71–79.
[27] D.S. Chaves, F.S. Frattani, M. Assafim, A.P. de Almeida, R.B. Zingali, S.S. Costa, Phenolic chemical composition of Petroselinum crispum extract and its effect on haemostasis, Nat. Prod. Commun. 6 (2011), 1934578X1100600709.
[28] S.R. Guntur, N.S. Kumar, M.M. Hegde, V.R. Dirisala, In Vitro Studies of the Antimicrobial and Free-Radical Scavenging Potentials of Silver Nanoparticles Biosynthesized From the Extract of Desmostachya bipinnata, Anal. Chem. Insights 13 (2018), 1177390118782877.
[29] M. Bindhu, M. Umadevi, Synthesis of monodispersed silver nanoparticles using Hibiscus cannabinus leaf extract and its antimicrobial activity, Spectrochim. Acta Part A Mol. Biomol. Spectrosc. 101 (2013) 184–190.
[30] M. Mohamed, N. Adbel-Ghani, O. El-Borady, M. El-Sayed, 5-Fluorouracil induces plasmonic coupling in gold nanospheres: new generation of chemotherapeutic agents, J. Nanomed. Nanotechol 3 (2012), 10.4172.
[31] L. Josimović, Study on some chemical changes in irradiated pepper and parsley, Int. J. Appl. Radiat. Isotopes 34 (1983) 787–791.
[32] M. Klekotko, K. Brach, J. Olesiak-Banska, M. Samoc, K. Matczyszyn, Popcorn-shaped gold nanoparticles: Plant extract-mediated synthesis, characterization and multiphoton-excited luminescence properties, Mater. Chem. Phys. 229 (2019) 56–60.
[33] S.S. Sana, L.K. Dogiparthi, Green synthesis of silver nanoparticles using Givotia moluccana leaf extract and evaluation of their antimicrobial activity, Mater. Lett. 226 (2018) 47–51.
[34] B.D. Lade, A.S. Shanware, Phytonanofabrication: Methodology and Factors Affecting Biosynthesis of Nanoparticles, Nanosystems, IntechOpen2020.
[35] D. Philip, Green synthesis of gold and silver nanoparticles using Hibiscus rosa sinensis, Physica E 42 (2010) 1417–1424.
[36] B. Bonigala, B. Kasukurthi, V.V. Konduri, U.K. Mangamuri, R. Gorrepati, S. Poda, Green synthesis of silver and gold nanoparticles using Stemona tuberosa Lour and screening for their catalytic activity in the degradation of toxic chemicals, Environ. Sci. Pollut. Res. 25 (2018) 32540–32548.
[37] E. Schreck, Y. Foucault, G. Sarret, S. Sobanska, L. Cécillon, M. Castrec-Rouelle, G. Uzu, C. Dumat, Metal and metalloid foliar uptake by various plant species exposed to atmospheric industrial fallout: mechanisms involved for lead, Sci. Total Environ. 427 (2012) 253–262.
[38] M. Hamelian, S. Hemmati, K. Varmira, H. Veisi, Green synthesis, antibacterial, antioxidant and cytotoxic effect of gold nanoparticles using Pistacia Atlantica extract, J. Taiwan Inst. Chem. Eng. 93 (2018) 21–30.
[39] J. Iqbal, B.A. Abbasi, T. Mahmood, S. Kanwal, R. Ahmad, M. Ashraf, Plant-extract mediated green approach for the synthesis of ZnONPs: Characterization and evaluation of cytotoxic, antimicrobial and antioxidant potentials, J. Mol. Struct. 1189 (2019) 315–327.
[40] M. Hamelian, K. Varmira, H. Veisi, Green synthesis and characterizations of gold nanoparticles using Thyme and survey cytotoxic effect, antibacterial and antioxidant potential, J. Photochem. Photobiol., B 184 (2018) 71–79.
[41] R. Venu, T. Ramulu, S. Anandakumar, V. Rani, C. Kim, Bio-directed synthesis of platinum nanoparticles using aqueous honey solutions and their catalytic applications, Colloids Surf. A 384 (2011) 733–738.
[42] S. Li, Y. Shen, A. Xie, X. Yu, L. Qiu, L. Zhang, Q. Zhang, Green synthesis of silver nanoparticles using Capsicum annuum L. extract, Green Chem. 9 (2007) 852–858.
[43] S.K. Chaudhuri, L. Malodia, Biosynthesis of zinc oxide nanoparticles using leaf extract of Calotropis gigantea: characterization and its evaluation on tree seedling growth in nursery stage, Appl. Nanoscience 7 (2017) 501–512.
[44] A. Muthuvel, K. Adavallan, K. Balamurugan, N. Krishnakumar, Biosynthesis of gold nanoparticles using Solanum nigrum leaf extract and screening their free radical scavenging and antibacterial properties, Biomed. Prevent. Nutrit. 4 (2014) 325–332.
[45] M.V. Sujitha, S. Kannan, Green synthesis of gold nanoparticles using Citrus fruits (Citrus limon, Citrus reticulata and Citrus sinensis) aqueous extract and its characterization, Spectrochim. Acta Part A Mol. Biomol. Spectrosc. 102 (2013) 15–23.
[46] N. Surovtseva, A. Eremenko, N. Smirnova, V. Pokrovskii, T. Fesenko, G. Starukh, The effect of nanosized titania-silica film composition on the photostability of adsorbed methylene blue dye, Theor. Exp. Chem. 43 (2007) 235–240.
[47] M. Rafique, I. Sadaf, M.B. Tahir, M.S. Rafique, G. Nabi, T. Iqbal, K. Sughra, Novel and facile synthesis of silver nanoparticles using Albizia procera leaf extract for dye degradation and antibacterial applications, Mater. Sci. Eng., C 99 (2019) 1313–1324.
[48] N. Cheval, N. Gindy, C. Flowkes, A. Fahmi, Polyamide 66 microspheres metallised with in situ synthesised gold nanoparticles for a catalytic application, Nanoscale Res. Lett. 7 (2012) 182.
[49] Y. Galagan, W.-F. Su, Reversible photoreduction of methylene blue in acrylate media containing benzyl dimethyl ketal, J. Photochem. Photobiol. A 195 (2008) 378–383.
[50] M. Haruta, N. Yamada, T. Kobayashi, S. Iijima, Gold catalysts prepared by coprecipitation for low-temperature oxidation of hydrogen and of carbon monoxide, J. Catal. 115 (1989) 301–309.
[51] I. Laoufi, M.-C. Saint-Lager, R. Lazzari, J. Jupille, O. Robach, S. Garaudée, G. Cabailh, P. Dolle, H. Cruguel, A. Bailly, Size and catalytic activity of supported gold nanoparticles: an in operando study during CO oxidation, J. Phys. Chem. C 115 (2011) 4673–4679.
[52] K.B. Narayanan, N. Sakthivel, Heterogeneous catalytic reduction of anthropogenic pollutant, 4-nitrophenol by silver-bionanocomposite using Cylindrocladium floridanum, Bioresour. Technol. 102 (2011) 10737–10740.
[53] V. Suvith, D. Philip, Catalytic degradation of methylene blue using biosynthesized gold and silver nanoparticles, Spectrochim. Acta Part A Mol. Biomol. Spectrosc. 118 (2014) 526–532.
[54] G.M. Sulaiman, W.H. Mohammed, T.R. Marzoog, A.A.A. Al-Amiery, A.A.H. Kadhum, A.B. Mohamad, Green synthesis, antimicrobial and cytotoxic effects of silver nanoparticles using Eucalyptus chapmaniana leaves extract, Asian Pacific J. Tropical Biomed. 3 (2013) 58–63.
[55] P. Velmurugan, M. Iydroose, S.-M. Lee, M. Cho, J.-H. Park, V. Balachandar, B.-T. Oh, Synthesis of silver and gold nanoparticles using cashew nut shell liquid and its antibacterial activity against fish pathogens, Indian J. Microbiol. 54 (2014) 196–202.
[56] S.-I. Yamagishi, T. Matsui, Nitric oxide, a janus-faced therapeutic target for diabetic microangiopathy—friend or foe?, Pharmacol. Res. 64 (2011) 187–194.
[57] G. Sathishkumar, P.K. Jha, V. Vignesh, C. Rajkuberan, M. Jeyaraj, M. Selvakumar, R. Jha, S. Sivaramakrishnan, Cannonball fruit (Couroupita guianensis, Aubl.) extract mediated synthesis of gold nanoparticles and evaluation of its antioxidant activity, J. Mol. Liq. 215 (2016) 229–236.
[58] J.K. Patra, K.-H. Baek, Novel green synthesis of gold nanoparticles using Citrullus lanatus rind and investigation of proteasome inhibitory activity, antibacterial, and antioxidant potential, Int. J. Nanomed. 10 (2015) 7253.
[59] J. Xie, J.Y. Lee, D.I. Wang, Y.P. Ting, Silver nanoplates: from biological to biomimetic synthesis, ACS Nano 1 (2007) 429–439.
[60] J.K. Patra, Y. Kwon, K.-H. Baek, Green biosynthesis of gold nanoparticles by onion peel extract: synthesis, characterization and biological activities, Adv. Powder Technol. 27 (2016) 2204–2213.
[61] E.L.H. Tang, J. Rajarajeswaran, S. Fung, M. Kanthimathi, Petroselinum crispum has antioxidant properties, protects against DNA damage and inhibits proliferation and migration of cancer cells, J. Sci. Food Agric. 95 (2015) 2763–2771.
[62] D. Tripathi, A. Modi, G. Narayan, S.P. Rai, Green and cost effective synthesis of silver nanoparticles from endangered medicinal plant Withania coagulans and their potential biomedical properties, Mater. Sci. Eng., C 100 (2019) 152–164.
[63] M. Gao, L. Sun, Z. Wang, Y. Zhao, Controlled synthesis of Ag nanoparticles with different morphologies and their antibacterial properties, Mater. Sci. Eng. C 33 (2013) 397–404.
[64] Z. Ni, X. Gu, Y. He, Z. Wang, X. Zou, Y. Zhao, L. Sun, Synthesis of silver nanoparticle-decorated hydroxyapatite (HA@ Ag) poriferous nanocomposites and the study of their antibacterial activities, RSC Adv. 8 (2018) 41722–41730.
[65] Y. Wu, Y. Yang, Z. Zhang, Z. Wang, Y. Zhao, L. Sun, A facile method to prepare size-tunable silver nanoparticles and its antibacterial mechanism, Adv. Powder Technol. 29 (2018) 407–415.
[66] I.A. Wani, T. Ahmad, Size and shape dependant antifungal activity of gold nanoparticles: a case study of Candida, Colloids Surf. B 101 (2013) 162–170.
[67] C. Vijilvani, M. Bindhu, F. Frincy, M.S. AlSalhi, S. Sabitha, K. Saravanakumar, S. Devanesan, M. Umadevi, M.J. Aljaafreh, M. Atif, Antimicrobial and catalytic activities of biosynthesized gold, silver and palladium nanoparticles from Solanum nigurum leaves, J. Photochem. Photobiol., B 202 (2020) 111713.
[68] V. Sunderam, D. Thiyagarajan, A.V. Lawrence, S.S.S. Mohammed, A. Selvaraj, In-vitro antimicrobial and anticancer properties of green synthesized gold nanoparticles using Anacardium occidentale leaves extract, Saudi J. Biolog. Sci. 26 (2019) 455–459.

[69] H. Schulz, M. Baranska, Identification and quantification of valuable plant substances by IR and Raman spectroscopy, Vib. Spectrosc. 43 (2007) 13–25.
[70] M. Sathishkumar, S. Pavagadhi, A. Mahadevan, R. Balasubramanian, Biosynthesis of gold nanoparticles and related cytotoxicity evaluation using A549 cells, Ecotoxicol. Environ. Saf. 114 (2015) 232–240.
[71] A.T. Khalil, M. Ovais, I. Ullah, M. Ali, Z.K. Shinwari, D. Hassan, M. Maaza, Sageretia thea (Osbeck.) modulated biosynthesis of NiO nanoparticles and their in vitro pharmacognostic, antioxidant and cytotoxic potential, Artif. Cells Nanomed. Biotechnol. 46 (2018) 838–852.